Green Chemistry

Cite this: *Green Chem.*, 2012, **14**, 338

www.rsc.org/greenchem

PAPER

Rh(I) complexes supported on a biopolymer as recyclable and selective hydroformylation catalysts†

Banothile C. E. Makhubela, Anwar Jardine and Gregory S. Smith*

Received 8th August 2011, Accepted 17th October 2011
DOI: 10.1039/c1gc15979h

Chitosan-supported Rh complexes were prepared in a stable form to form new catalysts and have been characterized using elemental analysis, UV-vis, FT-IR, ICP-MS, PXRD, solid state ^{31}P and ^{13}C NMR spectroscopy and TEM. Mononuclear Rh(I) complexes (as models for the heterogenized catalysts) were also prepared *via* the Schiff-base condensation reaction and the crystal structure of the cyclohexyl iminophosphine Rh(I) complex was elucidated. The chitosan-supported Rh complexes and mononuclear analogues are active catalysts in the hydroformylation of 1-octene with optimal reaction conditions realized at 75 °C and 30 bar syngas pressure. Under these conditions, 1-octene conversion to the desired linear aldehydes was observed and the best selectivity in this regard was shown by the supported iminophosphine-based rhodium catalyst. Overall, the supported catalysts showed similar chemo- and regioselectivities in comparison to their mononuclear counterparts but where more stable, being reused up to four times without loss of activity and selectivity.

1. Introduction

Hydroformylation has been widely used in industry for the production of aldehydes from alkenes since its discovery in 1938. An important example is the OXEA process (former Ruhrchemie/Rhône-Poulenc) which has been producing 8.0×10^5 tons of C4 and C5 aldehydes from propene or butene annually since 1984.[1] This process employs a $Rh/P(C_6H_4SO_3Na)_3$ (TPPTS) catalyst. Aldehydes are the starting material for making many useful secondary products such as i) alcohols (production of detergents) and ii) specialty chemicals (which are relevant to organic synthesis of fragrances and complex natural products).[1] In 1995, production capacity reached 6.6×10^6 tons. Over the past several decades, much effort has been directed toward the synthesis of highly active and selective catalysts for the hydroformylation reaction, using different transition metals.[1] The most commonly used catalysts for this reaction are based on Rh complexes due to their high activity and selectivity under milder conditions. It has been established that hydroformylation activity with regards to metal atom follows the trend: Rh≫Co≫Pt.[1b–d]

However, the practical application of homogeneous hydroformylation systems in industry has been limited by problems associated with separation of the catalyst/product mixture. Additionally, the process of separation by distillation is energy-intensive, time consuming and corrosive to equipment.[1b]

Consequently several approaches have been employed in solving this problem, such as aqueous biphasic, supported aqueous-phase, supported liquid-phase, supercritical fluids, ionic liquids and supported ionic liquid-phase catalysts.[1–6] Despite overcoming the separation challenge, these approaches often result in metal leaching and low regioselectivity to the aldehyde products. Alternatively, homogeneous catalysts have been immobilized on solid supports such as, dendritic scaffolds, polymers, metal oxides, mesoporous materials and various kinds of carbon.[7–10] However, these catalysts often suffer the drawbacks of reduced catalyst activity and irreproducibility.

Recently, researchers have looked to biopolymers as supports for transition metal catalysts due to their appealing abundance in nature, renewability, biodegradability and non-toxicity.[11] The use of several biopolymers like alignate, starch, gelatine, cellulose and chitosan have been reported in this regard.[11–15] Indeed, these efforts are leading to more cleaner and sustainable chemistry.

Chitosan (Fig. 1) can be produced by deacetylation of chitin, which is found in the exoskeleton of crustaceans and the cell walls of algae.[11] Scientists have reported its interesting antifungal, biopesticidal and anti-cancer properties, as well as its applications in food and water treatment.[16]

This material has shown encouraging potential as a solid support for the immobilization of transition metal catalysts owing to its affinity for metal ions and high thermal stability.[11] The amine groups of chitosan can be easily modified to create

Department of Chemistry, University of Cape Town, Rondebosch 7701, Cape Town, South Africa. E-mail: Gregory.Smith@uct.ac.za

† Electronic supplementary information (ESI) available: CCDC reference number 838557. For ESI and crystallographic data in CIF or other electronic format see DOI: 10.1039/c1gc15979h

Table 1 Microanalyses, loadings and yields of compounds (**1–4**)

Compound	Elemental analyses (%)				Ligand or Rh loading (mmol g^{-1})		
	C	H	N	C/N	EA	UV	Yield (%)[d]
Chitosan	40.92	6.02	7.85	5.21	2.10[a]	—	—
(**1**)	44.63	5.92	6.44	6.93	0.12[a]	0.12[b]	69
(**2**)	46.47	5.89	10.39	4.47	0.15[a]	0.13[b]	84
(**3**)	39.42	4.12	4.35	9.06	0.14[c]	—	85
(**4**)	38.47	4.91	5.77	8.05	0.09[c]	—	94

[a] Free NH_2 (accessible and inaccessible) determined by microanalysis.[18a,d,20a] [b] Determined using UV (absorbance is dependent on conc, solvent and pH [22]). [c] Determined using ICP-MS. [d] Yield by mass.

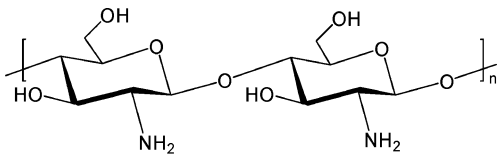

Chitosan

Fig. 1 Idealized structures of chitosan.

ligand donor sites for effective and stable metal coordination. As such, several examples of chitosan-Schiff base catalysts have been reported including those containing Cu, Pd and Co.[17–19] Recently, we reported the preparation of new chitosan-iminophosphine Pd catalysts for carbon-carbon cross-coupling reactions.[20a] The catalysts displayed high activity and yields that were comparable or better than those obtained using a similar homogeneous catalyst. As part of our continuing effort to extend a wide utility of the chitosan-Schiff base ligands, Rh has been complexed to these immobilized ligands forming the first examples of chitosan-iminopyridyl and -iminophosphine Rh complexes. Previously, it has been reported that an unmodified chitosan-Rh catalyst was used for 1-hexene hydroformylation reactions, however no metal leaching and catalyst recyclability studies were reported.[8e] We now report the preparation, characterization and evaluation in 1-octene hydroformylation using these new supported catalysts. This work draws upon some of the principles of green chemistry, such as atom economy and the use of a biodegradable and non-toxic biopolymer support. Furthermore, model mononuclear Rh homogeneous catalysts have been synthesized and characterized to compare their hydroformylation activity with their heterogenized counterparts.

2. Results and discussion

2.1 Catalyst synthesis and characterization

2.1.1 Heterogenized catalysts. Chitosan-supported Rh catalysts (**3** and **4**) were readily prepared by treatment of chitosan-Schiff base ligands (**1** and **2**)[20a] with $[RhCl(CO)_2]_2$. Thus, a mixture of the corresponding chitosan-Schiff base ligand (loading value: 0.12 mmol g^{-1} (**1**) and 0.13 mmol g^{-1} (**2**)) and an excess amount of $[RhCl(CO)_2]_2$ was stirred in dry acetone at room temperature (Scheme 1). The supported catalysts (**3** and **4**) were obtained in good yields as stable light-orange

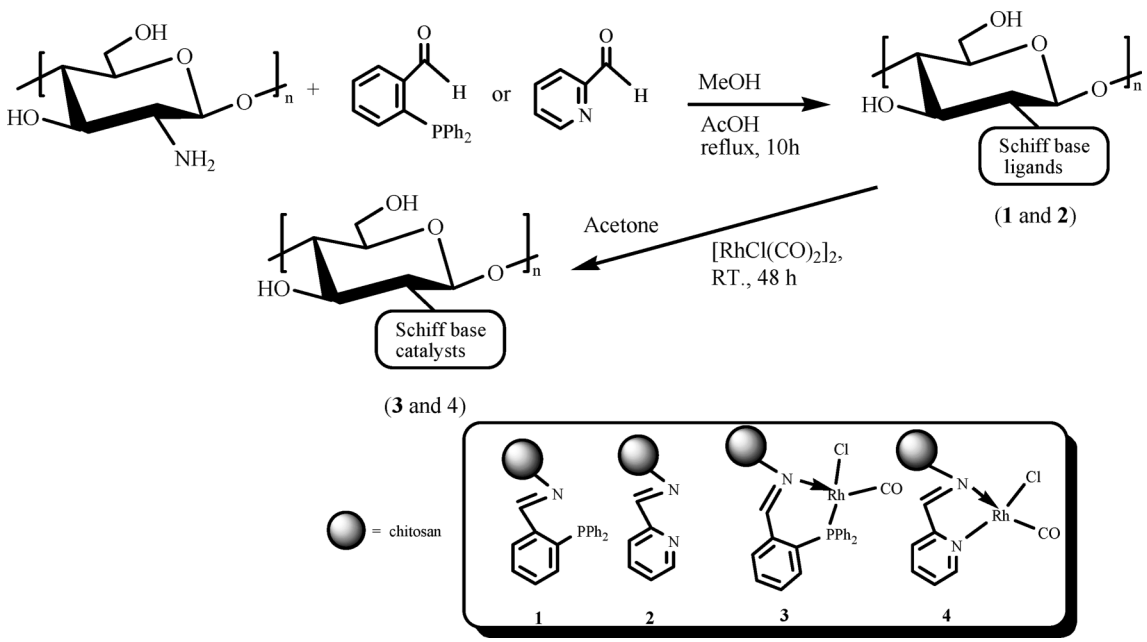

Scheme 1 Outline for the preparation of supported Schiff base ligands (**1** and **2**) and supported catalysts (**3** and **4**).

and purple solids respectively. They have been characterized by microanalysis, FT-IR, UV-vis, solid state ^{31}P and ^{13}C NMR spectroscopy, ICP-MS, PXRD and TEM. Using these methods the proposed structure of the chitosan Schiff base ligands (**1** and **2**) [20a] and chitosan-supported Rh catalysts (**3** and **4**) have been verified to be as described in Scheme 1 with the consideration of random anchoring.

The partial complexation of Rh to the supported Schiff base ligands was supported by microanalysis results, which indicated changes in the percentage of C, H and N when moving from the supported ligands (**1** and **2**) to the catalysts (**3** and **4**) (Table 1). ICP-MS results confirmed Rh loading values amounting to 0.145 mmol g^{-1} (**3**) and 0.092 mmol g^{-1} (**4**). These are slightly higher than those previously reported for analogous chitosan-supported Pd catalysts, possibly implying that the biopolymer has a stronger affinity to Rh.[20a]

IR absorption bands at 1640 cm^{-1} (**3**) and 1650 cm^{-1} (**4**) (1591 cm^{-1} for the pyridyl imine) were observed for the imine (C═N) vibrations together with terminal carbonyl bands at 1998 cm^{-1} (**3**) and 2003 cm^{-1} (**4**). The existence of one carbonyl band suggests that one isomer is preferred for the supported molecular Rh complexes (ESI **Fig. i**†).

UV-vis studies conducted on catalysts (**3** and **4**) as glycerol mulls revealed absorbance peaks at 319 nm and 348 nm for **3** and **4** respectively. These are in a similar range to those of their homogenous analogues (see Scheme 2) 322 nm (**5**) and 342 nm (**6**) (ESI **Fig. ii**†). These similar though weak absorbances observed by UV-vis supports the presence of molecular Rh complexes on the chitosan.[2,20a]

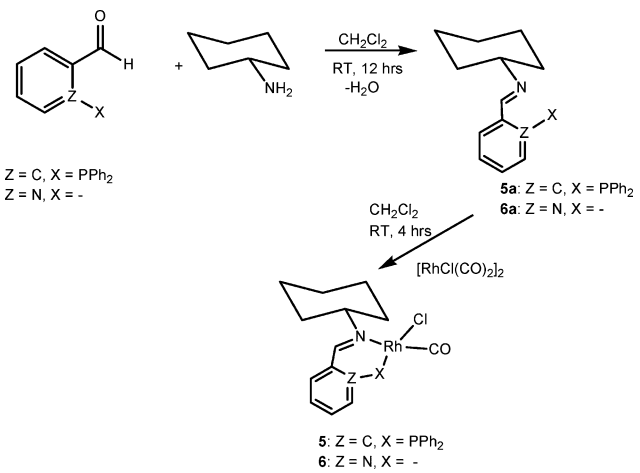

Scheme 2 Outline for the preparation of Schiff base ligands (**5a** and **6a**) and Rh(I) complexes (**5** and **6**).

TEM is widely used for the elucidation of morphology, particle size and shape as well as distribution and has proven very useful in this application.[7–10] The particle sizes of catalysts **3** and **4** were observed from TEM images to be spherically shaped nano-sized particles with sizes in the ranges of 3–7 nm (**3**) and 4–8 nm (**4**) (Fig. 2). They are uniformly dispersed across the biopolymer support and mostly equidistant. Rh particles visible through TEM imaging may imply intermolecular interactions of vicinal angstrom sized molecular Rh^{I} sites on the biopolymer resulting in nanosized particles. Willocq *et al.* have also seen Pd and Ru particles of size range 2–6 nm on phosphine modified

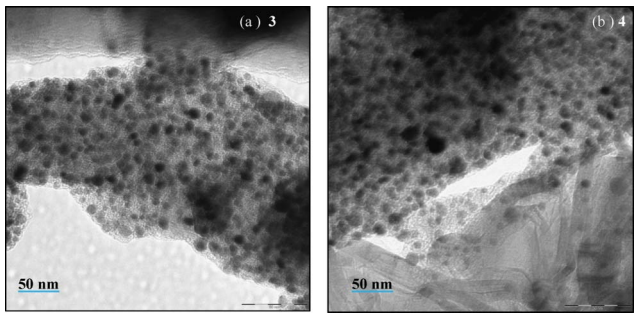

Fig. 2 TEM images of supported catalysts (a) **3** and (b) **4**.

active carbon, in which surface coordination of Pd and Ru organometallic complexes was achieved through the phosphines on the active carbon support.[21]

The crystallinity of the supported catalysts was examined by powder X-ray diffraction (Fig. 3). No Rh peaks were observed in the diffractograms of supported catalysts (**3** and **4**), meaning that the Rh particles are not composed of single crystallites. However, specific chitosan peaks (2θ = 15° and 25°) were evident on the diffractograms of both supported catalysts thus displaying high crystallinity of the chitosan support and that the basic structure of the chitosan is not hindered during preparation of the supported catalysts.

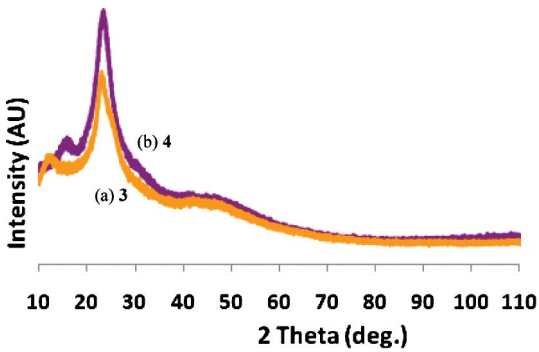

Fig. 3 Powder X-ray diffraction diagrams of a chitosan-supported Rh catalyst (a) **3** and (b) **4**.

Solid state ^{31}P NMR spectroscopy of the precursor chitosan-iminophosphine ligand (**1**) showed a signal at δ −18.5 ppm (Fig. 4a). This further indicates that the ligand has been successfully anchored to the chitosan support as this shift corresponds with the chemical shift obtained for the soluble ligand (**5a**) seen at δ −13.0 ppm. A peak due to phosphine oxide was also present at δ 35.0 ppm.[20b] The dimeric complex $[RhCl(CO)_2]_2$ was reacted with the chitosan-iminophosphine. The solid state ^{31}P NMR spectrum of the resulting supported complex (**3**) showed a decrease in intensity of the peak at δ −18.5 ppm, and the appearance of a peak at δ 56.6 ppm assigned to the Rh complex (Fig. 4b). This effect was previously observed in similar phosphine-Rh complexes attached to a peptide synthesis resin [20c] and $[RhCl(PPh_3)_3]$ immobilized on phosphinated MCM-41. These NMR experiments indicated that there are changes in the chitosan structure upon forming the chitosan-supported Schiff base ligand (**1**) and subsequent complex formation. To this effect, we have reason to believe molecular Rh(I) complexes do exist on the chitosan support, and it would thus be fair

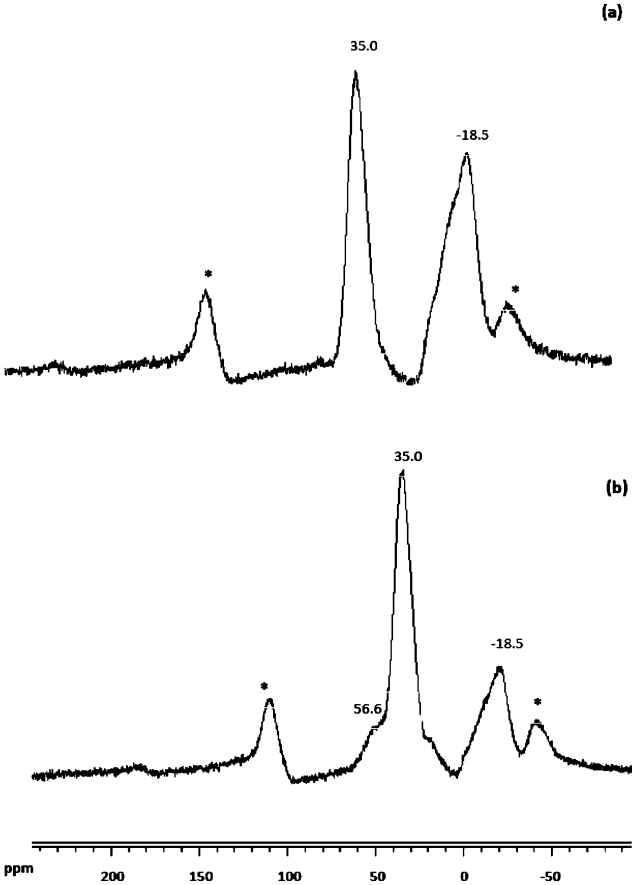

Fig. 4 Solid state ^{31}P NMR spectra of (a) chitosan-iminophosphine ligand (**1**) and (b) chitosan-supported Rh complex (**3**). ^{31}P one-pulse experiments were performed on a Bruker AMX 400 spectrometer at a ^{31}P frequency of 15 kHz at room temperature. Chemical shifts were referenced to Na_2HPO_4 at $\delta = 0$ ppm. Signals arising from side bands are marked with and an asterisk (*).

to assume the same for the chitosan-supported iminopyridyl catalyst (**4**).

The solid state ^{13}C NMR spectrum of the chitosan-supported iminophosphine ligand (**1**) evidenced successful anchoring of the iminophosphine ligand by the signal due to the imine carbon at $\delta = 174.0$ ppm as well as a signal for the aromatic carbons at $\delta = 131.0$ ppm (ESI **Fig. iii**(a)†). There is a slight drop in intensity of C_2 and C_4 carbons upon complexation of the Rh (ESI **Fig. iii**(b)†). This phenomenon strongly suggests possible spatial interactions of the coordinated complex with C_2 and C_4 of the chitosan backbone. Thus, further evidence of subtle structural modification of the chitosan can be seen on proceeding from chitosan-supported iminophosphine ligand (**1**) to chitosan-supported Rh complex (**3**).

2.1.2. Homogeneous catalysts. In addition, mononuclear analogues of chitosan-supported Rh(I) complexes (**5** and **6**) were prepared by the reaction of cyclohexyl-2-(diphenylphosphino)imine and cyclohexyl-2-iminopyridyl ligands (**5a** and **6a**) with $[RhCl(CO_2)]_2$ in dichloromethane (Scheme 2). The products were isolated in good yields (84% and 89%) as air and moisture stable bright orange and purple crystalline solids, respectively. Complex **5** decomposed without melting at 220 °C while **6** displayed a melting range of 182–185 °C. These new complexes (**5** and **6**) have been characterized by microanalysis, FT-IR, ^{1}H and ^{31}P NMR spectroscopy, single X-ray diffraction and mass spectrometry.

Microanalysis results for complexes (**5** and **6**) were in agreement with the calculated percentage CHN. Strong absorption bands, assigned to the imine C=N functionality were observed at 1625 cm^{-1} (**5**) and 1626 cm^{-1}(**6**) (pyridyl imine occurs at 1609 cm^{-1} in complex (**6**)).

Evidence for the coordination of the Rh metal center was seen through a shift from 1628 cm^{-1} in the cyclohexyl-2-(diphenylphosphino)imine ligand (**5a**) to 1625 cm^{-1} in complex (**5**). Similarly a shift from 1646 cm^{-1} in the cyclohexyl-2-pyridyimine ligand (**6a**) to 1626 cm^{-1} in complex (**6**) was observed. Single very strong carbonyl (C≡O) absorption bands at 1993 cm^{-1} and 1995 cm^{-1} suggested one preferred isomer in complexes (**5** and **6**) respectively.

NMR spectroscopy supported coordination of the cyclohexyl-2-(diphenylphosphino)imine ligand (**5a**) in a chelating manner to form a Rh(I) complex. This was seen in the shifting of two resonance signals in the ^{1}H NMR spectra. The signal due to the methine proton displayed an upfield shift from δ 8.73 ppm in (**5a**) to δ 8.27 ppm in the Rh complex (**5**). Furthermore, the protons on the carbon adjacent to the imine nitrogen showed a downfield shift from δ 3.03 ppm to δ 4.53 ppm. ^{31}P NMR spectroscopy showed coordination of phosphorus to Rh when the singlet observed in the cyclohexyl-2-(diphenylphosphino)imine ligand (**5**) (δ −13.45 ppm), shifted further downfield (δ 48.20 ppm) and appeared as a doublet with coupling constant 165 Hz in the spectrum of complex (**5**). This is consistent with Rh–P coupling.[23] For complex (**6**), a shifting of the methine proton resonance from δ 8.51 ppm in (**6a**) to δ 8.35 ppm in (**6**) was seen as well as a downfield shift of the protons on the carbon adjacent to the imine nitrogen from δ 3.41 ppm to δ 4.53 ppm. ESI-mass spectrometry further confirmed the integrity of the complexes by displaying base peaks at m/z 502.1 and 318.92 representing the $[M\text{-}Cl]^+$ ions for complexes **5** and **6** respectively.

Single crystals of complex (**5**) were obtained by slow evaporation from dichloromethane : *n*-hexane.[24,25a] An ORTEP drawing of complex (**5**) with the corresponding labelling scheme is shown in Fig. 5 together with selected bond lengths and angles. The molecular structure shows a 4-coordinate square-planar geometry around the Rh center, with the terminal carbonyl group *trans* to the imine functionality. The geometric parameter around the Rh atom are comparable with those found in similar complexes [RhCl(PyP)(CO)] (PyP = 1-(2-diphenylphosphino)ethyl parazole)[25b] and [RhCl(P–N)(CO)] (P–N = 2-(diphenylphosphino)propylimine.[23] The angle P(1)–Rh(1)–Cl(1) (171.327(1)°) is not the expected 180° indicating some distortion, possibly imposed by the 6-membered chelate ring about the Rh atom. This effect is also seen to cause deviation of the angle N(1)–Rh(1)–P(1) (84.91(4)°) from 90°.

2.2 Catalytic studies

The potential of the chitosan-supported and mononuclear Rh complexes (**3–6**) to catalyse the hydroformylation reaction were evaluated using 1-octene as the substrate (eqn (1)). The conversions of 1-octene were monitored by GC and in general

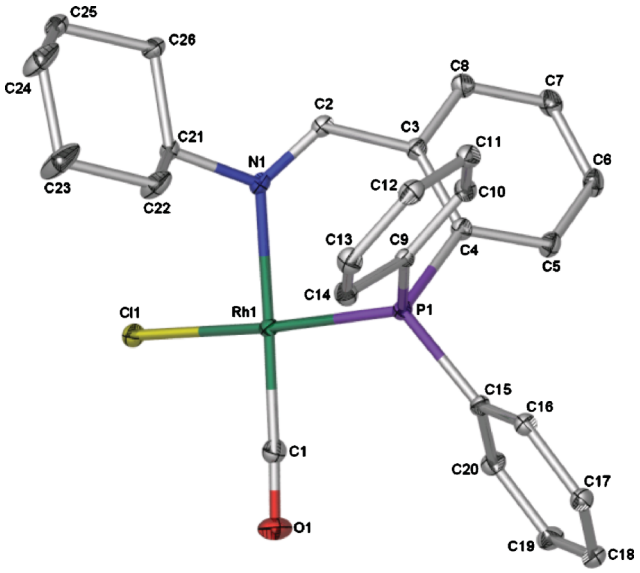

Fig. 5 Molecular structure of the mononuclear Rh^{I} iminophosphine complex (**5**) showing ellipsoids at the 50% probability level with hydrogen atoms omitted for clarity. Selected bond lengths (Å) and angles (°): Rh(1)–Cl(1) 2.4028(4), Rh(1)–N(1) 2.1318(13), Rh(1)–P(1) 2.2016(4), Rh(1)–C(1) 1.8261(16), N(1)–C(2) 1.2823(19), N(1)–C(21) 1.4927(18), P(1)–Rh(1)–Cl(1) 171.327(14), C(1)–Rh(1)–N(1) 178.71(6), N(1)–Rh(1)–P(1) 84.91(4), C(1)–Rh(1)–P(1) 95.68(5), C(1)–Rh(1)–Cl(1) 87.95(5), N(1)–Rh(1)–Cl(1) 91.62(4), C(2)–N(1)–C(21) 119.29(13).

products formed at optimal conditions were aldehydes (n : iso) by hydroformylation as well as some amounts of internal *iso*-octenes (*cis* and *trans* 2- and 3-octene) by isomerisation. No hydrogenation products were observed.

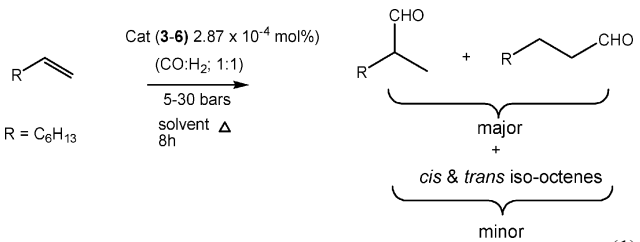

(1)

The chitosan supported catalysts (**3** and **4**) displayed similar reaction rates (Fig. 6) and conversions after 8 h. The mononuclear analogues also exhibited similar reaction rates and conversions with all catalysts displaying steady increase patterns.

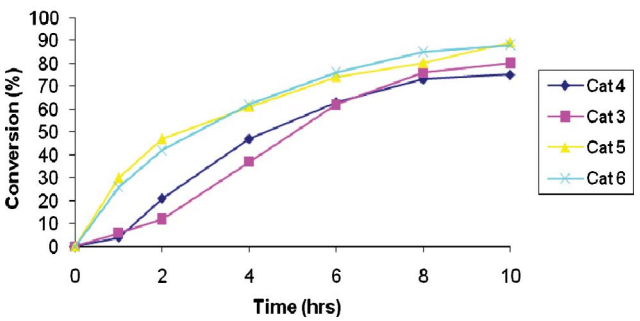

Fig. 6 Percentage conversion of 1-octene over 8 h using catalysts (**3–6**), data collected at 75 °C and 30 bar. (Average error estimate: (**3**) = ± 0.12; (**4**) = ± 0.11; (**5**) = ± 0.17 and (**6**) = ± 0.10).

The supported catalysts (**3** and **4**) displayed low to no activity over the first 2 h indicative of an induction period required to ensure diffusion of the syngas into the solvent followed by accessing the Rh sites on the chitosan. In contrast to that, the mononuclear analogues showed a higher catalytic rate over the first 4 h. Similar differences in the rate of conversion between homogeneous and catalysts supported on SBA-15 have been reported.[7c]

2.2.1 Effect of pressure. At $T = 75$ °C and syngas pressure = 5 bar, hydroformylation of 1-octene gave poor conversions to predominantly *iso*-octenes (Fig. 7 and Table 2, entries 1–4). Upon increasing the syngas pressure to 10 bar, higher conversions of 1-octene were afforded, though more *iso*-octenes were formed here too (Table 2, entries 5–8). Good conversions of 1-octene to the desired linear aldehyde product was therefore seen at 30 bar and 75 °C using catalysts (**3–6**) (*vide infra*, Fig. 8b and 9a). The supported catalysts show swelling in aqueous ethanol solvent (1 : 1 ratio) however poor activity was observed due to low solubility of the long hydrocarbon chain of the 1-octene substrate in aqueous medium. Hydroformylation of shorter chain α-olefins may yield better results.[26]

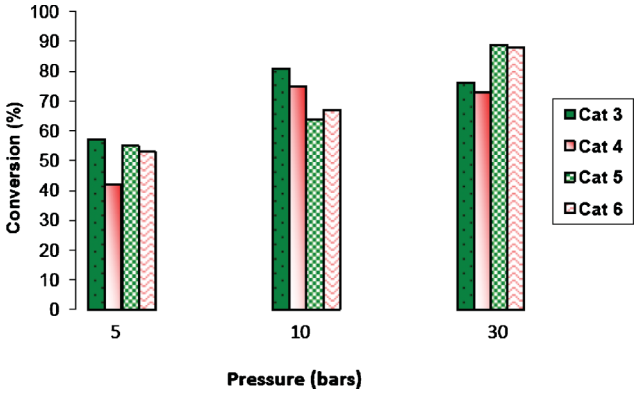

Fig. 7 Percentage conversion of 1-octene over 8 h using catalysts (**3–6**) at 75 °C. (Average error estimate: (**3**) = ± 0.11; (**4**) = ± 0.12; (**5**) = ± 0.16 and (**6**) = ± 0.11).

2.2.2 Effect of temperature. Hydroformylation of 1-octene was carried out at various temperatures using catalysts (**3–6**) (T = 55, 75 and 95 °C, Syngas pressure = 30 bar) (Fig. 8a–c). Reactions carried out at 55 °C saw very low conversions of 1-octene to *iso*-octenes exclusively with pyridylimine-based catalysts (**4** and **6**), while iminophosphine-based catalysts (**3** and **5**) formed almost equal amounts of aldehydes and *iso*-octenes. At 95 °C, high conversions of 1-octene were observed to initially *iso*-octenes (monitored by GC) which were converted to aldehydes over time (8 h). Thus at this temperature, more branched aldehydes are formed *via* hydroformylation of *iso*-octenes (Fig. 9b). The optimal temperature at which good conversion (TOF = 261–111 and TON = 2088 (**3**)) to desired linear aldehydes was found to be 75 °C. At this temperature iminophosphine-based catalysts (**3** and **5**) exhibited superior selectivity for nonanal than their pyridylimine-based counterparts, reiterating reports that bulky aryl phosphine ligands influences regioselectivity (Fig. 9a–b).[27a–b] Additionally, at T = 75 °C and syngas pressure = 30 bar the supported catalysts (**3** and **4**) showed almost similar

Table 2 Data for the hydroformylation of 1-octene at different pressures, after 8 h[a]

Entry	Cat.	Syngas press. (bar)	% Conversion	% Aldehyde	% *iso*-octenes	n : iso	TOF (h^{-1})[d]
1	**3**	5	57	10	90	43 : 57[b]	26
2	**4**	5	42	0	100	—	0
3	**5**	5	55	4	96	62 : 38[c]	10
4	**6**	5	53	2	98	64 : 36[c]	5
5	**3**	10	81	28	72	45 : 55[b]	75
6	**4**	10	75	5	95	70 : 30[b]	13
7	**5**	10	64	30	70	48 : 52[c]	78
8	**6**	10	67	25	75	52 : 48[c]	65

[a] Reactions carried out with ($CO : H_2$) (1 : 1) at 75 °C in xylene (10 ml) with 6.37 mmol of 1-octene and 2.87×10^{-3} mmol Rh catalyst (loading = 0.145 (**3**); 0.092 (**4**) mmol g^{-1}) (Error estimate: (**3**) = ± 0.10; (**4**) = ± 0.13; (**5**) = ± 0.16 and (**6**) = ± 0.12). GC conversions obtained using *n*-decane as an internal standard in relation to authentic standard *iso*-octenes and aldehydes. [b] Regioselectivity calculated at 2 h. [c] Regioselectivity calculated at 4 h. [d] TOF = (mol product/mol cat.) x h^{-1}.

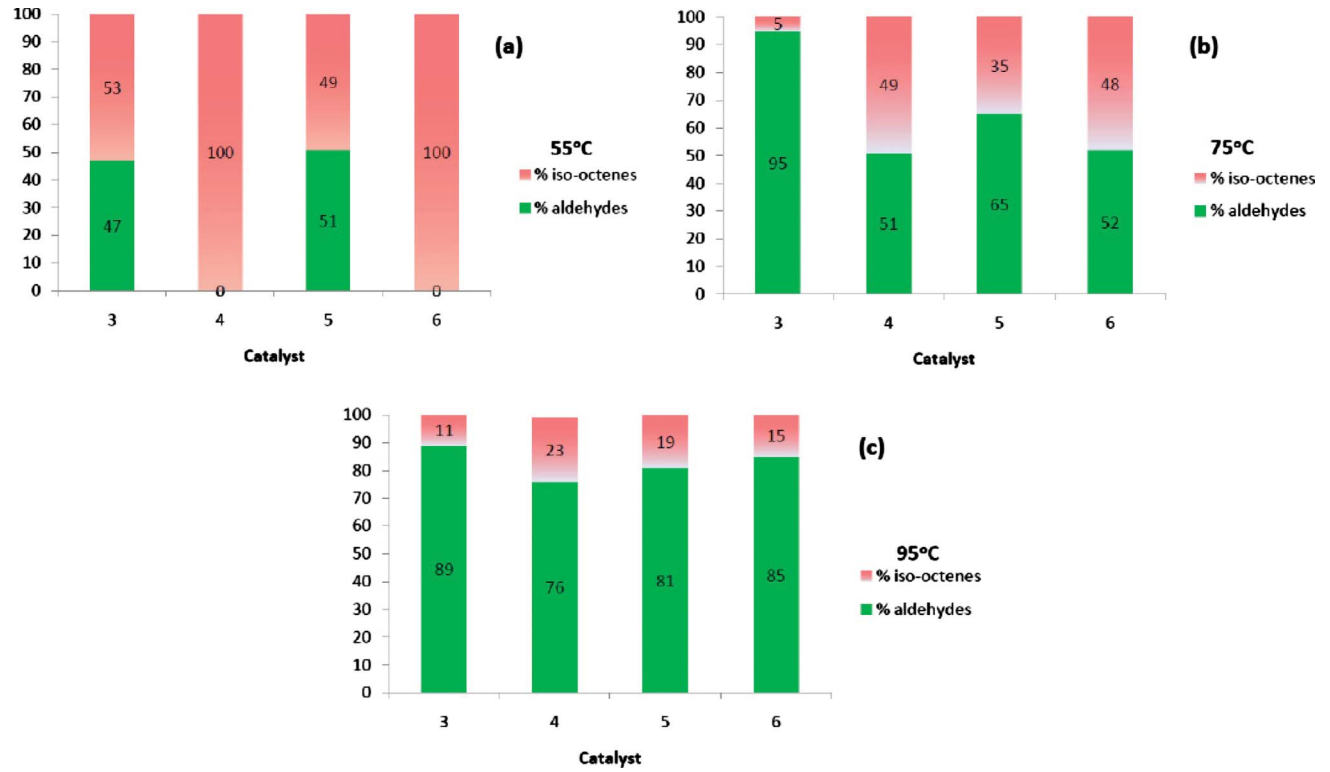

Fig. 8 Effect of temperature on chemoselectivity in hydroformylation of 1-octene using catalysts (**3–6**) at (a) 55 °C, (b) 75 °C and (d) °C.[27c] (Average error estimate: (**3**) = ± 0.10; (**4**) = ± 0.12; (**5**) = ± 0.15 and (**6**) = ± 0.13).

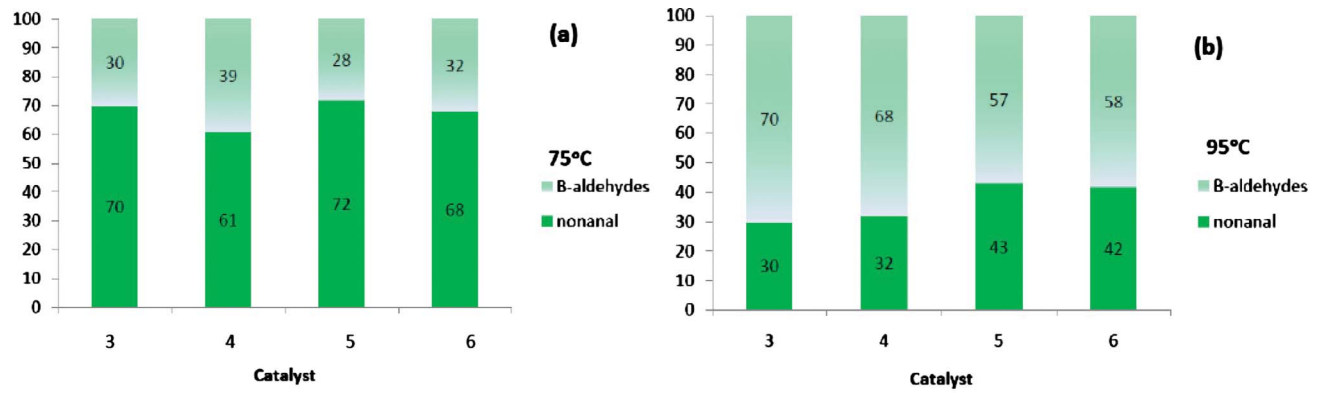

Fig. 9 Effect of temperature on regioselectivity in hydroformylation of 1-octene using catalysts (**3–6**) at (a) 75 °C and (b) 95 °C.[27c] (Average error estimate: (**3**) = ± 0.10; (**4**) = ± 0.11; (**5**) = ± 0.14 and (**6**) = ± 0.11).

chemo- and regioselectivities implying that the biopolymer backbone has no impact on selectivity during hydroformylation (*vide infra*).

2.2.3 Chemo- and regioselectivities. For the established optimal conditions (T = 75 °C, Syngas pressure = 30 bar), the catalysts showed moderate to high (for catalyst (**3**)) chemoselectivity for aldehyde products (52–95%) with some amounts of *iso*-octenes (Fig. 8b). Thus, in forming aldehyde products, these reactions are in line with the green chemistry principle of atom economy. Overall, catalysts (**3–6**) favoured formation of *iso*-octenes at low temperature (55 °C) and pressures (5 and 10 bar) as has been previously reported. When compared to [$Rh(CO)_2$(acac)] under similar conditions the current catalyst (**3–6**) show better regioselectivity.[28a]

In general, the catalysts (**3–6**) showed regioselectivity toward linear aldehydes (nonanal) at optimal conditions, with the iminophosphine-based catalysts (**3** and **5**) displaying superior selectivity for nonanal (70 and 72% respectively) than iminopyridyl-based catalysts (**4** and **6**) (57 and 68% respectively). Formation of branched aldehydes *via* preformed *iso*-octenes was mostly favoured at syngas pressure = 10 bar, T = 75 °C and syngas pressure = 30 bar, T = 95 °C. These observations can in future be exploited in the formation of chiral aldehydes, which are highly sought after in the pharmaceutical industry.[28b–d] Furthermore, the n : iso ratio of aldehydes obtained with supported catalysts (**3** and **4**) was similar to when mononuclear analogues (**5** and **6**) were employed effectively proving that the inherent chirality of the biopolymer support does not influence the catalytic behaviour around the active Rh centres. However, the support does play a crucial stabilizing role in catalyst (**3**) allowing for this catalyst to be recycled and reused (up to four times) while mononuclear analogues (**5** and **6**) decomposed to black species during reaction (*vide infra*). The chemo- and regioselectivity and activity displayed by the iminophosphine-based supported and mononuclear catalysts (**3** and **5**) compete well with related Rh supported and mononuclear catalysts in literature operated under higher conditions of temperature and pressure (ranging from: 80–175 °C and 50–90 bar).[29]

2.2.4 Rh leaching tests. A hot filtration test, whereby the supported catalysts (**3** and **4**) were filtered off 2 h into the reaction and the filtrates taken back to reaction did not stop catalytic conversion of 1-octene (Fig. 10). Notably, the filtrates did not show further hydroformylation of 1-octene under otherwise identical experimental conditions. Thus, 0.02% (in catalyst (**3**)) and 0.05% (in catalyst (**4**)) of Rh leached into solution, as determined by ICP-MS, and this minimally catalyses isomerisation.[30] This implies that chitosan-supported Rh complexes are the true active catalysts for the hydroformylation reaction, while a combination of Rh complexes and colloidal particles are responsible for isomerisation.[30]

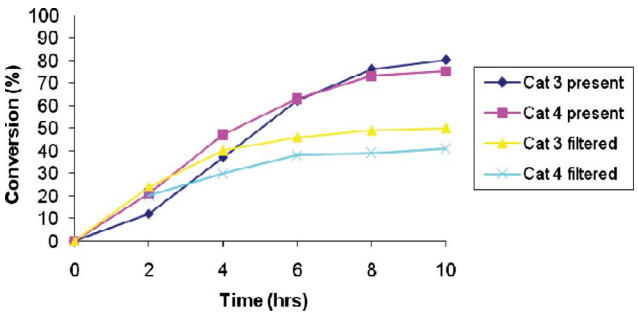

Fig. 10 Effect of removing supported Rh catalysts (**3** and **4**) from reaction (hot filtration test, (catalyst (**3** and **4**) removed after 2 h). (Average error estimate: (**3**) = ± 0.12; (**4**) = ± 0.11).

2.2.5 Catalyst reusability. The supported catalyst (**3**) was recycled four times with consistent conversion of 1-octene (75–79%) to mainly aldehydes.[31a] Catalyst deactivation may be due to sintering as was seen in similar Pd catalysts.[20a] Notably, chemo- and regio- selectivity was maintained throughout the cycles (average n : iso = 70 : 30). Catalyst (**4**) gave poor conversion (4%) on the second cycle indicative of the inferior stability of this catalyst compared to the iminophosphine-based catalyst (**3**). The iminophosphine-based catalysts exhibit slightly better activity in general. This may be attributed to the bulky phosphine ligand imposing a more favourable bite angle for the substrate (1-octene) or the formation of a more stable active species based on hard and soft acid and base principles.[31b]

3. Experimental

3.1 Materials and instrumentation

Low molecular weight chitosan (Cat. No. 44,886-9, deacetylation 75–85%, average molecular weight of < 6000 units), analytical grade cyclohexyl amine, 2-pyridine carboxaldehyde and 2(diphenylphosphino) benzaldehyde were purchased from Sigma Aldrich and used as received. All solvents were obtained commercially and distilled under N_2 prior to use. Methanol, ethanol, dichloromethane and acetone were dried over calcium hydride. $RhCl_3 \cdot 3H_2O$ was obtained from Johnson Matthey. $[RhCl(CO)_2]_2$[32] and chitosan-Schiff base ligands[20a] were prepared according to literature procedures.

UV-vis spectra were obtained at ambient temperature using a Varian Cary 50 Conc. UV-vis spectrophotometer as glycerol mulls. Powder X-ray diffraction (PXRD) data was collected on a Bruker D8 Advanced diffractometer (Co-Kα-radiation, λ = 1.78897 Å). IR spectra were recorded in KBr disks on a Perkin–Elmer Spectrum One FT-IR spectrometer. Melting points were determined using a Kofler hot stage microscope (Riechart Thermover). Elemental analyses were conducted with a Thermo Flash 1112 Series CHNS-O Analyzer. Electrospray Ionisation (ESI) mass spectrometry was carried out on a Waters API Quattro Micro triple quadrupole mass spectrometer in the positive-ion mode. Electron Impact mass spectrometry was conducted on a JEOL GCMATE II mass spectrometer. Inductively coupled plasma-mass spectrometry was obtained using a Perkin–Elmer Elan600 quadrupole ICP-MS with a Cetax LSX-200 UV laser module. TEM imaging was done on a JEOL 1200EXII CRYO TEM. Catalysis products were analysed using a Varian 3900 GC. ^1H and ^{31}P NMR spectra were recorded on a Varian XR400 MHz spectrometer using tetramethylsilane (TMS) as the internal standard (for ^1H) and H_3PO_4 as the external standard (for ^{31}P).

3.2. General procedure for the synthesis of chitosan-Schiff base Rh(I) catalysts (3 and 4)

The appropriate chitosan-Schiff base ligand was stirred with $[RhCl(CO)_2]_2$, in acetone at room temperature over 48 h. After the reaction, the supported Schiff base catalysts were collected by filtration, "conditioned" by refluxing in ethanol for 10 h in order to remove unreacted Rh, washed with distilled water, ethanol and acetone (50 ml each), and then dried under vacuum at 60 °C for 8 h.

3.2.1. Preparation of chitosan-2-(diphenylphosphino)imine-Rh catalyst (3). Chitosan-2-(diphenylphosphino)imine (350 mg, 0.035 mmol) was treated with a solution of $[RhCl(CO_2)]_2$ (40 mg, 0.105 mmol) in dry acetone (30 ml) at room temperature. After 48 h the product was obtained by filtration, "conditioned" by refluxing in ethanol for 10 h and washed thoroughly with water, ethanol and acetone (50 ml each) respectively. The light orange solid was then dried under vacuum at 60 °C for 8 h. Yield, (299 mg, 85%). FT-IR (KBr) ν_{max}/cm^{-1}: 3434 (s) (OH), (m) 2913 (C–H), 2003 (s) (C≡O), 1640 (s) (C=N), 1575 (m) (aromatic C=C), (br, s) 1154–1071 (pyranose), (s) 895 (aromatic C–H). Elemental Analysis: Found C, 40.47; H, 4.62; N, 4.35. ICP-MS: (Rh, mmol g^{-1}): 0.145

3.2.2. Preparation of chitosan-2-pyridylimine-Rh catalyst (4). Chitosan-2-pyridylimine (500 mg, 0.025 mmol) was treated with a solution of $[RhCl(CO_2)]_2$ (29 mg, 0.075 mmol) in dry acetone (40 ml) at room temperature. After 48 h the product was obtained by filtration, "conditioned" by refluxing in ethanol for 10 h and washed thoroughly with water, ethanol and acetone (50 ml each) respectively. The purple solid was then dried under vacuum at 60 °C for 8 h. Yield, (488 mg, 94%). FT-IR (KBr) ν_{max}/cm^{-1}: 3435 (s) (OH), (m) 2917 (C–H), 1998 (s) (C≡O), 1650 (s) (C=N), 1591 (m) (pyr. C=N), 1570 (m) (aromatic C=C), (br, s) 1152–1070 (pyranose), (s) 776 (aromatic C–H). Elemental Analysis: Found C, 46.47; H, 5.91; N, 5.77. ICP-MS: (Rh, mmol g^{-1}) 0.092

3.3. Preparation of cyclohexyl-2-(diphenylphosphino)imine ligand (5a)

Cyclohexyl amine (211 mg, 2.13 mmol) in CH_2Cl_2 (25 ml) was treated with 2-(diphenylphosphino) benzaldehyde (493 mg, 1.70 mmol) over 12 h at room temperature. After 12 h anhydrous magnesium sulfate was transferred to the stirred solution and the mixture was filtered, the solvent was removed by rotary evaporation to give a light yellow solid for compound (**5a**), which was dried under vacuum for 2 h. Yield, (630 mg, 92%). mp.: 98–99 °C. FT-IR (KBr) ν_{max}/cm^{-1}: 2923 (s) (C–H), 1628 (s) (C=N), 1584 (m) (aromatic C=C), 695 (s) (aromatic C–H). δ_H (400 MHz; DMSO-d_6, Me_4Si) 8.73 (1H, d, imine, $^4J_{PH}$ = 4.4 Hz), 7.86 (1H, m, **Ar**), 7.21–7.66 (12H, br m, **Ar**), 6.77 (1H, m, **Ar**), 3.03 (1H, t, **H**CN=), 0.99–1.78 (10H, br m, C**H**$_2$). δ_P (121 MHz; DMSO-d_6; H_3PO_4) –13.01 (s). Elemental analysis: Found C, 79.33; H, 7.06; N, 2.13 $C_{25}H_{26}NP$ requires: C, 80.84; H, 7.06, N, 3.77. EI-MS: m/z 370.7, (M-H^+, 100%).

3.4. Preparation of cyclohexyl-2-(diphenylphosphino)imine rhodium(I) complex (5)

$[RhCl(CO_2)]_2$ (78 mg, 0.202 mmol) in CH_2Cl_2 (20 ml) was added to a solution of cyclohexyl-2(diphenylphosphino)imine ligand (**5a**) (150 mg, 0.404 mmol) in CH_2Cl_2 (15 ml) and this stirred at room temperature. After 4 h, the solvent was removed by rotary evaporation to afford a bright orange solid which was purified by column chromatography as follows: a solution of the crude product in CH_2Cl_2 (10 ml) was passed through a silica packed column and eluted with ethyl acetate. The product associated with the bright orange band was collected, the solvent removed by rotary evaporation and the bright orange crystalline solid product (**5**) was isolated and dried under vacuum for 3 h. Single crystals of complex (**5**) were obtained by slow evaporation from CH_2Cl_2 : *n*-hexane (1 : 1) Yield, (178 mg, 82%). mp., decomposes without melting at the onset of 220 °C. FT-IR (KBr) ν_{max}/cm^{-1}: 2930 (s) (C–H), 1993 (vs) (C≡O), 1625 (s) (C=N), 1563 (m) (aromatic C=C), 696 (s) (aromatic C–H). δ_H (400 MHz; DMSO-d_6, Me_4Si) 8.27 (1H, s imine), 7.87 (1H, m, **Ar**), 7.36–7.71 (12H, br m, **Ar**), 6.83 (1H, m, **Ar**), 4.53 (1H, t, 1H, **H**CN =), 0.98–1.97 (10H, br m, C**H**$_2$). δ_P (121 MHz; DMSO-d_6; H_3PO_4) 48.20 (d, $^1J_{RhP}$ = 165 Hz). Elemental analysis: Found C, 58.69; H, 4.94; N, 2.39, $C_{26}H_{26}Cl_2NOPRh$. requires: C, 58.06; H, 4.87, N, 2.60. EI-MS: m/z 502.1, (M-Cl^+, 99%).

3.5. Preparation of cyclohexyl-2-pyridylimine ligand (6a)

Cyclohexyl amine (2.0 g, 20.17 mmol) in CH_2Cl_2 (35 ml) was reacted with 2-pyridinecarboxaldehyde (1.72 g, 16.08 mmol) over 12 h at room temperature. After 12 h anhydrous magnesium sulphate was transferred to the stirred solution and the mixture was filtered, the solvent was removed by rotary evaporation to give a viscous yellow oil for compound (**6a**), which was dried under vacuum for 2 h. Yield, (2.2 g, 73%). FT-IR (KBr) ν_{max}/cm^{-1}: 2910 (s) (C–H), 1646 (s) (C=N), 1609 (m) (pyr. C=N), 1566 (m) (aromatic C=C), 744 (s) (aromatic C–H). δ_H (400 MHz; DMSO-d_6, Me_4Si) 8.58 (1H, m, **Ar**), 8.51 (1H, s, imine), 7.90 (1H, t, $^3J_{HH}$ = 7.7 Hz **Ar**), 7.70 (1H, m, **Ar**), 7.48 (1H, m, **Ar**), 3.41 (1H, m, **H**CN =), 1.02–1.88 (br m, 10H, C**H**$_2$). Elemental analysis: Found C, 76.24; H, 8.22, N, 14.07 $C_{12}H_{16}N_2$ requires: C, 76.55; H, 8.34, N, 14.28. ESI-MS: m/z 180.02, (M-8H^+, 100%).

3.6. Preparation of cyclohexyl-2-pyridylimine rhodium(I) complex (6)

$[RhCl(CO_2)]_2$ (200 mg, 0.516 mmol) in CH_2Cl_2 (15 ml) was added to a solution of cyclohexyl-2-pyridylimine ligand (**6a**) (186 mg, 1.030 mmol) in CH_2Cl_2 (20 ml) and this stirred at room temperature. After 4 h, the solvent was removed by rotary evaporation to afford a purple solid of complex (**6**) which was dried under vacuum for 3 h. Yield, (250 mg, 89%). **mp.**: 182–185 °C. FT-IR (KBr) ν_{max}/cm^{-1}: 2935 (s) (C–H), 1626 (s) (C=N), 1597 (m) (pyr. C=N), 1566 (m) (aromatic C=C), 778 (s) (aromatic C–H). δ_H (400 MHz; DMSO-d_6, Me_4Si): 8.89 (1H, m, **Ar**), 8.35 (1H, s, imine), 8.25 (1H, t, ^3J = 7.6 Hz **Ar**), 8.00 (1H, m, **Ar**), 7.68 (1H, m, **Ar**), 4.01 (1H, m, **H**CN=), 0.99–1.86 (10H, br m, 10H, C**H**$_2$) Elemental analysis: Found C, 44.61; H, 4.25; N, 7.17. $C_{13}H_{16}ClN_2ORh$ requires:

C, 44.03; H, 4.55, N, 7.90, ESI-MS: m/z 318.92, (M-Cl$^+$, 98%).

3.7 General hydroformylation procedure

Hydroformylation reactions were conducted in a 90 ml stainless steel autoclave. The autoclave was charged with xylene (10 ml), 1-octene (715 mg, 6.37 mmol), *n*-decane internal standard (180 mg, 1.26 mmol) and one of the Rh catalysts (**3**, **4**, **5** or **6**) (2.87 $\times 10^{-3}$ mmol, substrate: Rh ratio = 2276 : 1). The autoclave was flushed three times with syngas ($CO:H_2$, 1 : 1 ratio) followed by pressurizing and heating to the desired syngas pressure and temperature respectively. Samples were taken every 2 h and analysed using gas chromatography (GC). The products were confirmed in relation to authentic *iso*-octenes and aldehydes.

4. Conclusions

Two new supported-Rh(I) catalysts based on a sustainable, biodegradable and non-toxic biopolymer support have been successfully prepared in a stable form. They were characterized using several techniques including elemental analysis, UV-vis, FT-IR, ICP-MS, ^{31}P and ^{13}C solid state NMR spectroscopy, TEM and PXRD. Model mononuclear model Rh(I) complexes of the chitosan-supported catalyst were also prepared and characterized using ^{1}H and ^{31}P NMR, UV-vis and FT-IR spectroscopy, mass spectrometry, elemental analysis and single X-ray crystallography.

All the catalysts were active in the hydroformylation of 1-octene under mild conditions with negligible amounts of Rh leaching into the solution. The activity as well as regio- and chemo-selectivity was affected by factors such as temperature and syngas pressure and under optimal conditions of 75 °C and 30 bar, good selectivity for nonanal was seen for both the supported and mononuclear catalysts. Iminophosphine-based catalyst (**3**) showed the best activity, chemoselectivity, regioselectivity as well as recyclability and can therefore be singled out for further development.

Acknowledgements

We would like to thank the University of Cape Town, the National Research Foundation of South Africa and NRF-DST Centre of Excellence in Catalysis (c*change) for financial support. A generous loan of rhodium trichloride from the AngloPlatinum Corporation/ Johnson Matthey is gratefully acknowledged.

References

1 (*a*) O. Roelen, *US Patent*, 2327066, 1943; (*b*) P. Eibracht, L. Barfacker, C. Buss, C. Hollmann, B. E. Kistsos-Rzychon, C. L. Kranemann, T. Rische, R. Roggenbuck and A. Schmidt, *Chem. Rev.*, 1999, **99**, 3329 and references therein; (*c*) B. Cornils, W. A. Herrmann, M. Rasch and M. Beller, *Angew. Chem., Int. Ed. Engl.*, 1994, **33**, 2144; (*d*) B. Cornils, C. D. Frohning and C. W. Kohlpaintner, *J. Mol. Catal. A: Chem.*, 1995, **104**, 17; (*e*) B. Cornils, W. A. Herrmann and R. W. Ecki, *J. Mol. Catal. A: Chem.*, 1997, **116**, 27; D. Evans, J. A. Osborn and G. Wilkinson, *J. Chem. Soc. A*, 1968, 13133; (*f*) P. W. N. M. van Leeuwen, C. Claver, *Rh-Catalyzed Hydroformylation*, Kluwer Academic, Dordrecht, 2000, pp. 6; (*g*) B. Cornils, W. A. Herrmann and M. Rasch, 'Otto Roelen, Pioneer in Industrial Homogeneous Catalysis, *Angew. Chem., Int. Ed. Engl.*, 1994, **33**, 2144; (*h*) H. Bricout, F. Hapiot, A. Ponchel, S. Tilloy and E. Monflier, *Sustainability*, 2009, **1**, 924; (*i*) B. Cornils, *Org. Process Res. Dev.*, 1998, **2**, 121.

2 (*a*) B. Cornils and E. Wiebus, *Chemtech.*, 1995, **25**, 33; (*b*) B. Cornils and E. G. Kuntz, *J. Organomet. Chem.*, 1995, **502**, 177.

3 (*a*) A. Riisager, K. M. Erikson, J. Hjortkjaer and R. Fehrmann, *J. Mol. Catal. A: Chem.*, 2003, **193**, 259–272; (*b*) M. E. Davis, in *Aqueous-Phase Organometallic Catalysis*, ed., B Cornils and W. A. Hermann, Chapter 4, 7 Wiley, Weinheim, 1998, pp. 241; (*c*) M. E. Davis, *Chemtech.*, 1992, **22**, 498.

4 (*a*) Z. K. Lopez-Castillo, R. Flores, I. Kani, J. P. Fackler Jr. and A. Akgerman, *Ind. Eng. Chem. Res.*, 2008, **42**, 3893; (*b*) C. Halm, M. J. Kurth and Angew, *Angew. Chem., Int. Ed.*, 1998, **37**, 510.

5 (*a*) J. S. Wilkes, *Green Chem.*, 2002, **4**, 73; (*b*) J. L. Anthony, E. J. Maginn and J. F. Brennecke, *J. Phys. Chem. B*, 2002, **106**, 7315; (*c*) J. S. Wilkes, *J. Mol. Catal. A: Chem.*, 2004, **214**, 11.

6 (*a*) A. Riisager, K. M. Eriksen, P. Wasserscheid and R. Fehrmann, *Catal. Lett.*, 2003, **98**, 149; (*b*) A. Riisager, R. Fehrmann, S. Flicker, R. Van Hal, M. Haumann and P. Wasserscheid, *Angew. Chem., Int. Ed.*, 2004, **43**, 2; (*c*) Y. Yang, C. Deng and Y. Yuan, *J. Catal.*, 2005, **232**, 108.

7 (*a*) P. Arya, N. Verugopal Rao and J. Singkhonrat, *J. Org. Chem.*, 2000, **65**, 1881; (*b*) R. Van Heerbeek, P. C. J. Kamer, P. W. N. M. van Leeuwen and J. N. H Reek, *Chem. Rev.*, 2002, **102**, 3717; (*c*) P. Li and S. Kawi, *J. Catal.*, 2008, **257**, 23.

8 (*a*) G. O. Evans, C. U. Pittman, R. Mc Millan, R. T. Beach and R. Jones, *J. Organomet. Chem.*, 1975, **87**, 189; (*b*) F. Shibahara, K. Nozaki, T. Matsuo and T. Hiyama, *Bioorg. Med. Chem. Lett.*, 2002, **12**, 1825; (*c*) F. Shabahara, K. Nozaki and T. Hiyama, *J. Am. Chem. Soc.*, 2003, **125**, 8555; (*d*) D. E. Bryant and M. Kilner, *J. Mol. Catal. A: Chem.*, 2003, **193**, 83; (*e*) E. V. Slivinskii and N. V. Kolesnichenko, *Russ. Chem. Bull.*, 2004, **53**, 2449.

9 (*a*) M. A. Valenzuela, G. Aguilar, P. Bosch, H. Armendariz, P. Salas and A. Montoya, *Catal. Lett.*, 1992, **15**, 179; (*b*) A. M. Trzeciak, J. J. Ziołkowski, Z. Jaworska-Galas, W. Mista and J. Wrzyszcz, *J. Mol. Catal.*, 1994, **88**, 13; (*c*) J. Wrzyszcz, M. Zawadzki, A. M. Trzeciak and J. J. Ziołkowski, *J. Mol. Catal. A: Chem.*, 2002, **189**, 203; (*d*) L. Huang and S. Kawi, *Catal. Lett.*, 2004, **92**, 57.

10 (*a*) J. P. K. Reynhardt, Y. Yang, A. Sayari and H. Alper, *Chem. Mater.*, 2004, **16**, 4095; (*b*) X. Lan, W. Zhang, L. Yan, Y. Ding, X. Han, L. Lin and X. Bao, *J. Phys. Chem. C*, 2009, **113**, 6589.

11 (*a*) E. Guibal, *Prog. Polym. Sci.*, 2005, **30**, 71; (*b*) B. F. Peirano, V. Thierry, F. Quignard, M. Rabitzer and E. Guibal, *J. Membr. Sci.*, 2009, **329**, 30; (*c*) D. J. Macquarrie and J. J. E. Hardy, *Ind. Eng. Chem. Res.*, 2005, **44**, 8499; (*d*) E. Guibal, V. Thierry and B. F. Peirano, *Ion Exch. Solvent Extr.*, 2007, **18**, 151; (*e*) S.-S. Yi, D.-H. Lee, E. Sin and Y.-S. Lee, *Tetrahedron Lett.*, 2007, **48**, 6771; (*f*) S. E. S. Leonhardt, A. Stolle, B. Ondruschka, G. Cravotto, C. De Leo, K. D. Jandt and T. F. Keller, *Appl. Catal., A*, 2010, **379**, 30.

12 W.-L. Wei, H.-Y. Zhu, C.-L. Zhao, M.-Y. Huang and Y.-Y. Jiang, *React. Funct. Polym.*, 2004, **59**, 33.

13 M. J. Gronnow, R. Luque, D. J. Macquarrie and J. H. Clark, *Green Chem.*, 2005, **7**, 552.

14 X. Zhang, Y. Geng, B. Han, M.-Y. Ying, M.-Y. Huang and Y. Y. Jiang, *Polym. Adv. Technol.*, 2001, **12**, 642.

15 K. R. Reddy, N. S. Kumar, P. S. Reddy, B. Sreedhar and M/L. Kantam, *J. Mol. Catal. A: Chem.*, 2006, **252**, 12.

16 (*a*) J. Linden, R. Stoner, K. Knustson, C. Gardner-Hughes, *Org. Disease Control Elicitors*, Agro Food Ind. Hi-Te, 2000, pp. 12; (*b*) S. F. Ausar, N. Passalacqua, L. F. Castagna, I. D. Bianco and D. M. Beltramo, *Int. Dairy J.*, 2002, **12**, 899; (*c*) Z. Guo, R. Xing, S. Liu, Z. Zhang, X. Ji, L. Wang and P. Li, *Carbohydr. Res.*, 2007, **342**, 1329; (*d*) R.-M. Wang, N.-P. Pe, P.-F. Song, Y.-F. He, L. Ding and Z.-Q. Lei, *Polym. Adv. Technol.*, 2009, **20**, 959; (*e*) R.-M. Wang, N.-P. Pe, P.-F. Song, Y.-F. He, L. Ding and Z. Lei, *Pure Appl. Chem.*, 2009, **81**, 2397.

17 (*a*) H. Wang, W. Sun and C. Xia, *J. Mol. Catal. A: Chem.*, 2003, **206**, 199; (*b*) J. E. dos Santos, E. R. Dockal and E. T. G. Cavalheiro, *Carb. Res.*, 2005, **60**, 277.

18 (*a*) J. J. E. Hardy, S. Hubert, D. J. Macquarrie and A. J. Wilson, *Green Chem.*, 2004, **6**, 53; (*b*) Y. Cui, L. Zhang, Y. Li and Polym, *Polym. Adv. Technol.*, 2005, **16**, 633; (*c*) X. Xu, P. Liu, S.-H. Li, P. Zhang and X.-Y. Wang, *React. Kinet. Catal. Lett.*, 2006, **88**, 217; (*d*) Y. A. Skorik, C. A. R Gomes, M. T. S. D. Vasconcelos and Y. G. Yatluk, *Carbohydr. Res.*, 2003, **338**, 271.

19 (*a*) J. Tong, Z. Li and C. Xia, *J. Mol. Catal. A: Chem.*, 2005, **231**, 197; (*b*) L.-X. Wang, Z.-W. Wang, G. S. Wang, X.-D. Lin and J.-G. Ren, *Polym. Adv. Technol.*, 2010, **21**, 244.

20 (*a*) B. C. E. Makhubela, A. Jardine and G. S. Smith, *Appl. Catal., A*, 2011, **393**, 231; (*b*) Z. Li, Q. Peng and Y. Yuan, *Appl. Catal., A*, 2003, **239**, 79; (*c*) S. R. Gilbertson, X. Wang, G. S. Hoge, C. A. Klug and J. Schaefer, *Organometallics*, 1996, **15**, 4678.

21 C. Willocq, S. Hermans and M. Devillers, *J. Phys. Chem.*, 2008, **112**, 5533.

22 K. Tømmeraas, S. P. Strand, W. Tian, L. Kenne and K. M. Vårum, *Carbohydr. Res.*, 2001, **336**, 291.

23 N. C. Antonels, B. Therrien, J. R. Moss and G. S. Smith, *Inorg. Chem. Commun.*, 2009, **12**, 716.

24 See ESI† **Section i**.

25 (*a*) L. J. Farrugia, *J. Appl. Crystallogr.*, 1997, **30**, 565; (*b*) S. Burling, L. D. Field, B. A. Messerle, K. Q. Vuong and P. Turner, *Dalton Trans.*, 2003, 4181.

26 E. G. Kuntz, *Chemtech.*, 1987, **14**, 570.

27 (*a*) C. K. Brown and G. Wilkinson, *J. Chem. Soc. A*, 1970, 2753; (*b*) D. Evans, G. Yaqupsky and G. Wilkinson, *J. Chem. Soc. A*, 1968, 3133; (*c*) See ESI† **Section ii**.

28 (*a*) N. C. Antonels, J. R. Moss and G. S. Smith, *J. Organomet. Chem.*, 2011, **696**, 2003; (*b*) A. D. Worthy, C. L. Joe, T. E. Lightburn and K. L. Tan, *J. Am. Chem. Soc.*, 2010, **132**, 14757; (*c*) T. E. Lightburn, O. A. Paolis, K. H. Cheng and K. L. Tan, *Org. Lett.*, 2011, **13**, 2686; (*d*) H. Fernández-Pèrez, P. Etayo, A. Panossian and A. Vidal-Ferran,, *Chem. Rev.*, 2011, **111**, 2119.

29 (*a*) W. Zhou and D. He, *Green Chem.*, 2009, **11**, 1146; (*b*) M. M. Taquikhan, S. B. Halligudi and S. H. R. Abdi, *J. Mol. Catal.*, 1988, **45**, 215; (*c*) T. Mathivet, C. Mèliet, Y. Castanet, A. Mortreux, L. Caron, S. Tilloy and E. Monflier, *J. Mol. Catal. A: Chem.*, 2001, **176**, 105; (*d*) D. U. Parmar, H. C. Bajaj, S. D. Bhatt and R. V. Jasra, *Bulletin of the Catal. Soc. Of India*, 2003, **2**, 34–39; (*e*) L. Leclercq, M. Sauthier, Y. Castanet, A. Mortreux, H. Bricout and E. Monflier, *Adv. Synth. Catal.*, 2005, **347**, 55; (*f*) C. C. Miyagawa, J. Kupka and A. Schumpe, *J. Mol. Catal. A: Chem.*, 2005, **234**, 9; (*g*) M. Bortenschlager, N. Schöllhorn, A. Wittmann and R. Weberskirch, *Chem.–Eur. J.*, 2007, **13**, 520; (*h*) J. A. Bae, K.-C. Song, J.-K. Jeon, Y. S. Ko, Y.-K. Park and J.-H. Yim, *Microporous Mesoporous Mater.*, 2009, **123**, 289; (*i*) J. D. Scholten and J. Dupont, *Organometallics*, 2008, **27**, 4439; (*j*) S. Dastgir, K. S. Coleman, A. R. Cowley and M. L. H. Green, *Dalton Trans.*, 2009, 7203; (*k*) W. Zhou, Y. Li and D. He, *Appl. Catal., A*, 2010, **377**, 114; (*l*) G. M. Pawar, J. Weckesser, S. Blechert and M. R. Buchmeiser, *Beilstein J. Org. Chem.*, 2010, **6**, 1; (*m*) S. Dastgir, K. S. Coleman and M. L. H. Green, *Dalton Trans.*, 2011, **40**, 661; (*n*) R. M. Deshpande, A. A. Kelkar, A. Sharma, C. Julcour-Lebigue and H. Delmas, *Chem. Eng. Sci.*, 2011, **66**, 1631; (*o*) M. T. Zarka, M. Bortenschlager, K. Wurst, O. Nuyken and R. Weberskirch, *Organometallics*, 2004, **23**, 4817.

30 See ESI† **Section iii (Table a)**.

31 (*a*) See ESI† **Section iv (Table b)**; (*b*) R. G. Pearson, *J. Am. Chem. Soc.*, 1963, **85**, 3533.

32 A. J. Deeming and P. J. Sharratt, *J. Organomet. Chem.*, 1975, **99**, 447.